THE TRUE NATURE OF THE EQUILIBRIUM FOR GEOSTATIONARY OBJECTS, APPLICATIONS TO THE HIGH AREA-TO-MASS RATIO DEBRIS

Fabien Gachet, Alessandra Celletti, Giuseppe Pucacco — University of Rome 'Tor Vergata'

Christos Efthymiopoulos — Academy of Athens

ABSTRACT

The long-term dynamics of the geostationary (GEO) region has been studied both numerically [1, 2] and analytically [3, 4, 5, 6], and some of these results contributed to the IADC guidelines for disposal of objects in the GEO region.

In this work, we revisit the dynamics of this region through the application of canonical perturbation theory, and we apply our results to study the peculiar dynamical behavior of high area-to-mass ratio space debris. More specifically, previous works focused on the evolution of objects *around* a nominal solution called the forced equilibrium solution. Here, instead we focus on the nature of the equilibrium solution itself. Thanks to a higher order normal form, we demonstrate that this equilibrium is actually a lower dimensional object containing slow frequencies. This means that even placed at this pseudo–equilibrium, an object will exhibit periodic variations of its elements, which can be large. We give an analytical expression of these variations, valid for long time scales.

To this end, we considered the Hamiltonian of the system accounting for all major perturbations in GEO : the Earth gravitational potential at order and degree 2, the third body perturbations from the Sun and the Moon from [7], and the solar radiation pressure. Using canonical perturbation theory, we perform a rigorous averaging of the 8 degrees of freedom Hamiltonian by the method of normal forms via Lie Series [8, 9]. The fast terms are then eliminated by a series of canonical transformation, revealing the long-period evolution of the different elements. This allows us to derive the forced equilibrium of this averaged Hamiltonian which is a lower dimensional object containing 5 slow frequencies defining a quasi-periodic orbit, which shows the actual nature of this pseudo–equilibrium. We obtain through a back-transformation of the canonical transformation made from the forced equilibrium, the analytical time-explicit evolution of all elements at this equilibrium. This analytical result is compared to the numerical integration of the full model before averaging, and gives satisfying accuracy. The long term evolution of the inclination and eccentricity for an object at the equilibrium are particularly analyzed showing strong dependence on the area-to-mass ratio.

We highlight that in addition to the geopotential at order and degree 2, we use a realistic model for the Sun and the Moon from [7], where the Moon and the Sun are on elliptical, inclined orbits with a variation of their argument of perigee and right ascension of the ascending node. As noted in [5], having a fixed Sun-Earth distance in the estimation of solar radiation pressure (an assumption made in some of the previous studies such as [4]) would induce spurious long-period terms in eccentricity and inclination evolution. This also ensures that the solar radiation pressure which derives from the position of the Sun is correctly modeled. Another novelty of the approach is that the Hamiltonian is derived in cylindrical coordinates since the geometry of the GEO region is very suitable for this coordinate system, therefore our approach does not need the disturbing function expansions making it simple to develop, and our results are directly translatable in Keplerian elements without singularity. The time-explicit solutions also give direct access to the equilibrium without scanning the whole phase space, and the long-term behavior described by these formulas can be used for disposal studies.

Index Terms— Space debris, high area-to-mass ratio objects, long-term dynamics, normal form, averaging

1. INTRODUCTION

As of 2015, more than 23% of the total mass of objects tracked by the US Strategic Command is in near GEO [10]. To safeguard the use of this orbit, end-of-life recommendations to dispose of spacecrafts in graveyard orbits beyond GEO that would not allow crossing with the ones of the functional satellites for at least a hundred years were proposed by the Inter-Agency Space Debris Coordination Committee (IADC) [11]. Prior to these, a number of mostly numerical studies derived the properties of long-term evolution of regular objects close to GEO [12]. The dynamics in this region are governed by the action of the low-order terms of the gravitational field of the Earth and the luni-solar third body gravitational perturbations [1, 2].

A new class of geostationary debris discovered a decade ago as reported in [13] reignited the need for dynamical studies in GEO : the high area-to-mass ratio (HAMR) objects. These objects have been identified as coming from thermal insulation layers wrapping certain components of satellites that could have been detached from defunct satellite breakups, or

from impact by smaller debris on satellites [14], and can have an apparent $\frac{A}{m}$ of $30m^2/kg$ [15]. They exhibit peculiar dynamical behavior compared to the regular, low area-to-mass ratio debris. Indeed, these HAMR objects' orbits can reach a very high eccentricity of 0.55 in a few years as observed in [16], mainly due to the action of the Solar radiation pressure (SRP), and their inclination can also reach higher values such as 30 to 40 degrees, while its associated period can decrease to less than 20 years. These phenomenon have been studied analytically by [3, 4, 5, 6, 17]. These studies show that, at GEO, the SRP modifies the equilibrium of the dynamical system in different ways. Concerning the inclination, the SRP induces a shift from the *forced inclination* (also called the inclination of the Laplace plane) around which libration takes place for low $\frac{A}{m}$ at about 7.4 deg, to higher values. This shift is directly dependent on $\frac{A}{m}$, as can be seen in [18, 4] where an analytical estimate of the shift is given. As for the eccentricity, the SRP causes large yearly variations around the *forced eccentricity* proportional to the value of $\frac{A}{m}$ that can be elegantly approximated by $e_{forced} \sim 0.01 \times C_r \, \frac{A}{m}$, where C_r is the reflectivity coefficicent.

2. MODEL

2.1. Assumptions of the model

In this work we consider a space debris orbiting the Earth at the geostationary distance and subject to the action of the following forces, which are given to some approximation as described below:

(i) the gravitation of the Earth, including the oblateness of the Earth provided by the spherical harmonic coefficient $C_{2,0}$ and by the first tesseral harmonics $C_{2,2}$ and $S_{2,2}$ representing the equatorial ellipticity of the Earth;

(ii) the third body perturbations due to the Moon and the Sun, whose potentials are expanded up to order 2 in the small ratio of the distance of the satellite to the third body, either Sun or Moon;

(iii) the Solar radiation pressure (hereafter SRP), using the *cannonball* approximation [19]. The SRP is approximated like for the third body perturbation due to the Sun. The influence of eclipses which shadow the satellite are not considered, since as shown in [20] they do not contribute significantly to the dynamics.

It is important to note that, at GEO, different perturbations end up having the same magnitude as can be seen in [21]. The Keplerian term of the Earth gravity is the major contributor, and by far, to the dynamics. But then, the perturbations due to the $C_{2,0}$ term, the Moon, the Sun, and the SRP for an $\frac{A}{m} = 1\,\mathrm{m}^2/\mathrm{kg}$ are of the same order of magnitude. If a regular area-to-mass ratio of $0.01\,\mathrm{m}^2/\mathrm{kg}$ for a satellite is considered, then the SRP is two orders of magnitude lower. However, if an even higher area-to-mass ratio is considered, such as $\frac{A}{m} = 10\,\mathrm{m}^2/\mathrm{kg}$, or up to $30\,\mathrm{m}^2/\mathrm{kg}$ as for some observed space debris, then the SRP becomes the first highest perturbation in magnitude. The magnitude of the other terms stemming from the Earth's gravitational field rapidly decreases as the distance of the debris from the Earth increases. For example, at GEO, the next harmonics $C_{3,3}$ and $S_{3,3}$ become two orders of magnitude smaller than $C_{2,2}$ and $S_{2,2}$. The above considerations lead us to support our choice of a model limited to the second order coefficients and including the relevant role that SRP might have in physically interesting cases.

To be completely exhaustive, other forces could be considered, such as the gravitational influence of Jupiter, the Earth's tides, the albedo of the Earth and the Moon, the interaction of the satellite with the magnetic field, etc. Due to their even smaller order of magnitude compared to the effects listed in (i)-(iii), they are neglected in the present work.

2.2. Hamiltonian model

As noted in Section 1, we use the Hamiltonian formalism to implement a normal form theory. The Hamiltonian associated with the model including the effects (i)-(iii) is defined by the sum of the kinetic energy and the potential in an inertial frame. To this end, we define a frame with origin at the barycenter of the Earth, the x-axis pointing to the Vernal equinox, the z-axis aligned with the axis of rotation of the Earth, pointing North, and the y-axis completing a right-handed framework.[1] When considering third body attraction such as from the Moon and the Sun, this frame is actually not inertial, since the Earth is attracted by those bodies, and therefore, its center of mass - to which the frame is attached - does not have a rectilinear uniform acceleration anymore. Let us note that the problem of the non-inertial reference frame is often dealt with by introducing fictitious forces in the third body perturbations, the so-called *indirect* contribution of the third bodies on the center of mass of the Earth. We follow this approach in section 2.4.

In this reference frame, the classical spherical coordinates are (r, θ, Φ), where r is the distance from the center of the Earth to the object, θ the colatitude measured positively from the z-axis, and $\Phi = \phi + \Omega_\oplus t$ is the longitude measured positively from the x-axis, where $\Omega_\oplus$ is the angular velocity of the Earth about its own axis of rotation in the inertial space. In this study we consider $\Omega_\oplus$ constant and precisely equal to $7.292\,115\,854\,834\,04 \times 10^{-5}\,\mathrm{rad/s}$.

We also define a more practical frame, where the definition of the geopotential is simpler: an Earth centered, Earth fixed reference frame. This frame is defined from our previous frame of reference as having a constant rotation about

[1] We do not consider the movement of Earth's rotational axis, since it is an extremely small effect with a period of 25 770 years; in most cases, this equinoctial precession of the Earth affects the dynamics on time scales longer than the time frame considered in the present study.

the z-axis, equal to $\Omega_\oplus$. We attach the usual spherical coordinates (r, θ, ϕ) to this uniformly rotating frame of reference, the first two quantities being identical to those in the previous frame, and ϕ being the longitude counted positive westward from Greenwich.

The spherical coordinates were introduced for clarity for the reader as they are used in the classical definition of the geopotential but let us finally introduce the classical cylindrical coordinates, which will be the main set of coordinates throughout the paper. They indeed fit well the geometry of the geostationary ring as pointed out in the introduction. Here are the transformations used from spherical to cylindrical coordinates:

$$\begin{aligned} \rho &= r \sin\theta \\ \varphi &= \phi \\ z &= r \cos\theta, \end{aligned} \tag{1}$$

where ρ is the planar radius, φ is the longitude (identical to ϕ), and z is the altitude.

The Hamiltonian function associated to the model described by the effects (i)-(iii) is the sum of the total kinetic energy T and the potential energy U, including the indirect effects of the luni-solar perturbations as explained above. We have $U = mV$, with V the potential per unit mass. The kinetic energy can be written as

$$T = \frac{1}{2} m \left(\dot{\rho}^2 + \rho^2 \dot{\Phi}^2 + \dot{z}^2 \right) , \tag{2}$$

where m is the mass of the considered body. The momenta conjugated to the coordinates r, θ, Φ are given by

$$\begin{aligned} p_\rho &= m\dot{\rho} \\ p_\Phi &= m\rho^2 \dot{\Phi} \\ p_z &= m\dot{z} \, . \end{aligned} \tag{3}$$

Without loss of generality, from now on we shall consider a unitary mass. Therefore, the Hamiltonian *per unit mass* can be expressed (without changing the definition of the momenta) as

$$\begin{aligned} H &= H(\rho, \Phi, z, p_\rho, p_\Phi, p_z, t) = T + V \\ &= \frac{{p_\rho}^2}{2} + \frac{{p_\Phi}^2}{2\rho^2} + \frac{p_z^2}{2} + V(\rho, \Phi, z, t) \, , \end{aligned} \tag{4}$$

where V represents the potential derived from all forces accounted for in the model, and depends actually on ϕ instead of Φ as shown in (5). The dependence on time of the Hamiltonian is dealt with in section 2.6.

We will now examine the expression of the potential for the different perturbations we take in account.

2.3. The geopotential

The dynamics of an object orbiting the Earth must take into account the gravitational influence of our planet, whose potential can be expanded in spherical harmonics [22] up to order and degree 2 in the (r, θ, ϕ) coordinate system as :

$$\begin{aligned} V_{GEO_2} = \\ &- \frac{\mu_\oplus}{\sqrt{\rho^2 + z^2}} + \frac{\sqrt{5}\bar{C}_{2,0}\mu_\oplus R_\oplus^2}{2(\rho^2+z^2)^{3/2}} - \frac{3\sqrt{5}\bar{C}_{2,0}\mu_\oplus R_\oplus^2 z^2}{2(\rho^2+z^2)^{5/2}} \\ &+ \frac{\sqrt{15}\bar{C}_{2,2}\mu_\oplus R_\oplus^2 z^2 \cos(2\varphi)}{2(\rho^2+z^2)^{5/2}} - \frac{\sqrt{15}\bar{C}_{2,2}\mu_\oplus R_\oplus^2 \cos(2\varphi)}{2(\rho^2+z^2)^{3/2}} \\ &+ \frac{\sqrt{15}\mu_\oplus R_\oplus^2 \bar{S}_{2,2} z^2 \sin(2\varphi)}{2(\rho^2+z^2)^{5/2}} - \frac{\sqrt{15}\mu_\oplus R_\oplus^2 \bar{S}_{2,2} \sin(2\varphi)}{2(\rho^2+z^2)^{3/2}} \end{aligned} \tag{5}$$

where $\mu_\oplus = \mathcal{G} m_\oplus$ with $\mathcal{G}$ is the gravitational constant, $m_\oplus$ and $R_\oplus$ the mass and equatorial radius of the Earth, $P_{n,m}$ are the associated Legendre polynomials, $\bar{C}_{n,m}$, $\bar{S}_{n,m}$ are the normalized spherical harmonic coefficients. The physical values of the coefficients are given in Table 1. Note that the coefficients of degree 1 are 0 since the center of mass is at the origin of the coordinate system, and the coefficients of degree 2 and order 1 are 0 since the z axis is aligned with the rotation of the Earth in our model.

Table 1: Values of $\bar{C}_{n,m}, \bar{S}_{n,m}$ in units of 10^{-6} up to degree and order 2, from NASA EGM96 [23].

n	m	$\bar{C}_{n,m}$	$\bar{S}_{n,m}$
2	0	484.165371736	0
2	2	2.43914352398	1.40016683654

2.4. The luni-solar perturbation

The luni-solar perturbation is described by the following potential, which includes the indirect terms mentioned in section 2.2 (second terms in the sums):

$$V_{\mathbb{C}} = -\mathcal{G} m_{\mathbb{C}} \left(\frac{1}{|\mathbf{r} - \mathbf{r}_{\mathbb{C}}|} + \frac{\mathbf{r} \cdot \mathbf{r}_{\mathbb{C}}}{|\mathbf{r}_{\mathbb{C}}|^3} \right) . \tag{6}$$

Similarly for the Solar potential we have:

$$V_\odot = -\mathcal{G} m_\odot \left(\frac{1}{|\mathbf{r} - \mathbf{r}_\odot|} + \frac{\mathbf{r} \cdot \mathbf{r}_\odot}{|\mathbf{r}_\odot|^3} \right) . \tag{7}$$

Both $\mathbf{r}_\odot$ and $\mathbf{r}_{\mathbb{C}}$ can be calculated as functions of time and we follow here the development of [7], with formulas truncated from series expansions at a low order, but still accurate to 0.1-1% for decades around the year 2000. We will recall all necessary formulas so that the paper is self contained and then introduce our notation used in the normal form procedure.

Remark: It is important to note that in [7] the given formulas are in the geocentric non-rotating EME2000 frame in which the x-axis points towards the mean equinox on 1 January 2000 at noon, where our geocentric non-rotating reference frame's x-axis points towards Greenwich. To transpose

the formulas to our reference frame, we perform a simple rotation taking in account the position of the Greenwich meridian at this date in the EME2000 frame.

We then multiply all vectors given in the EME2000 frame by the rotation matrix R_G:

$$R_G = \begin{pmatrix} \cos\Omega_G & \sin\Omega_G & 0 \\ -\sin\Omega_G & \cos\Omega_G & 0 \\ 0 & 0 & 1 \end{pmatrix} , \tag{8}$$

with $\Omega_G = 280.4606^\circ$ the position of the Greenwich meridian on 1 January 2000 at noon. We have first

$$\mathbf{r}_\odot = R_G \cdot \begin{pmatrix} r_\odot \cos\lambda_\odot \\ r_\odot \sin\lambda_\odot \cos\varepsilon \\ r_\odot \sin\lambda_\odot \sin\varepsilon \end{pmatrix} , \tag{9}$$

where $r_\odot$ is the Sun's distance, $\lambda_\odot$ its longitude, both in the EME2000 frame, and $\varepsilon = 23.439\,291\,11^\circ$ is the obliquity of the ecliptic. The time evolutions of $\lambda_\odot$ and $r_\odot$ (the latter measured in millions of kilometers) are given by the following truncated series expansions:

$$\begin{aligned} \lambda_\odot &= \Omega + \omega + M_\odot + 6892'' \sin M_\odot + 72'' \sin 2M_\odot \\ r_\odot &= 149.619 - 2.499 \cos M_\odot - 0.021 \cos 2M_\odot \end{aligned} \tag{10}$$

with Ω the right ascension of the ascending node, ω the argument of perihelion and $M_\odot$ the mean longitude of the Sun. Their values are:

$$\Omega + \omega = 282.9400^\circ , \quad M_\odot = \varphi_M + 357.5256^\circ , \tag{11}$$

with

$$\varphi_M = \Omega_M \cdot t , \tag{12}$$

and

$$\Omega_M = 35999.049^\circ/\text{centuries} , \tag{13}$$

being the yearly frequency with which the Sun revolves around the Earth and

$$t = \frac{JD - 2451545.0}{36525.0} \tag{14}$$

being the number of Julian centuries since 1 January 2000 at 12:00, with JD the Julian Date.

For the Moon, since its motion is more complex with respect to the Earth than that of the Sun, more terms are needed. We have:

$$\mathbf{r}_\leftmoon = R_G \cdot \begin{pmatrix} 1 & 0 & 0 \\ 0 & \cos\varepsilon & -\sin\varepsilon \\ 0 & \sin\varepsilon & \cos\varepsilon \end{pmatrix} \begin{pmatrix} r_\leftmoon \cos\lambda_\leftmoon \cos\beta_\leftmoon \\ r_\leftmoon \sin\lambda_\leftmoon \cos\beta_\leftmoon \\ r_\leftmoon \sin\beta_\leftmoon \end{pmatrix} , \tag{15}$$

where $r_\leftmoon$ is the Moon's distance, $\lambda_\leftmoon$ its longitude and $\beta_\leftmoon$ its latitude, both in the EME2000 frame. The time evolution of these quantities is represented by the following truncated series expansions:

$$\begin{aligned} r_\leftmoon &= (385000 - 20905\cos(l_\leftmoon) - 3699\cos(2D_\leftmoon - l_\leftmoon) \\ &\quad - 2956\cos(2D_\leftmoon) - 570\cos(2l_\leftmoon) \\ &\quad + 246\cos(2l_\leftmoon - 2D_\leftmoon) - 205\cos(l'_\leftmoon - 2D_\leftmoon) \\ &\quad - 171\cos(l_\leftmoon + 2D_\leftmoon) \\ &\quad - 152\cos(l_\leftmoon + l'_\leftmoon - 2D_\leftmoon))\ \text{km} \end{aligned} \tag{16}$$

$$\begin{aligned} \lambda_\leftmoon &= L_0 + 22640'' \sin(l_\leftmoon) + 769'' \sin(2l_\leftmoon) \\ &\quad - 4856'' \sin(l_\leftmoon - 2D_\leftmoon) + 2370'' \sin(2D_\leftmoon) \\ &\quad - 668'' \sin(l'_\leftmoon) - 412'' \sin(2F_\leftmoon) \\ &\quad - 212'' \sin(2l_\leftmoon - 2D_\leftmoon) - 206'' \sin(l_\leftmoon + l'_\leftmoon - 2D_\leftmoon) \\ &\quad + 192'' \sin(l_\leftmoon + 2D_\leftmoon) - 165'' \sin(l'_\leftmoon - 2D_\leftmoon) \\ &\quad + 148'' \sin(l_\leftmoon - l'_\leftmoon) - 125'' \sin(D_\leftmoon) \\ &\quad - 110'' \sin(l_\leftmoon + l'_\leftmoon) - 55'' \sin(2F_\leftmoon - 2D_\leftmoon) \end{aligned} \tag{17}$$

$$\begin{aligned} \beta_\leftmoon &= 18520'' \sin(F_\leftmoon + \lambda_\leftmoon - L_0 + 412'' \sin(2F_\leftmoon) \\ &\quad + 541'' \sin(l'_\leftmoon)) - 526'' \sin(F_\leftmoon - 2D_\leftmoon) \\ &\quad + 44'' \sin(l_\leftmoon + F_\leftmoon - 2D_\leftmoon) - 31\sin(-l_\leftmoon + F_\leftmoon - 2D_\leftmoon) \\ &\quad - 25\sin(-2l_\leftmoon + F_\leftmoon) - 23\sin(l'_\leftmoon + F_\leftmoon - 2D_\leftmoon) \\ &\quad + 21\sin(-l_\leftmoon + F_\leftmoon) + 11''\sin(-l'_\leftmoon + F_\leftmoon - 2D_\leftmoon) . \end{aligned} \tag{18}$$

where L_0 is the Moon's mean longitude, $l_\leftmoon$ is the Moon's mean anomaly, $l'_\leftmoon$ is the Sun's mean anomaly, $F_\leftmoon$ is the the mean angular distance of the Moon from the ascending node and $D_\leftmoon$ is the difference between the mean longitudes of the Sun and the Moon. We have:

$$\begin{aligned} L_0 &= \varphi_{M_p} + \varphi_{M_a} + 218.31617^\circ \\ l_\leftmoon &= \varphi_{M_a} + 134.96292^\circ \\ l'_\leftmoon &= M_\odot = \varphi_M + 357.52543^\circ \\ F_\leftmoon &= \varphi_{M_p} + \varphi_{M_a} + \varphi_{M_S} + 93.27283^\circ \\ D_\leftmoon &= \varphi_{M_p} + \varphi_{M_a} - \varphi_M + 297.85027^\circ \end{aligned} \tag{19}$$

with

$$\begin{aligned} \varphi_{M_a} &= \Omega_{M_a}\, t \\ \varphi_{M_p} &= \Omega_{M_p}\, t \\ \varphi_{M_S} &= \Omega_{M_s}\, t \end{aligned} \tag{20}$$

and

$$\begin{aligned} \Omega_{M_a} &= 477198.86753^\circ/\text{centuries} \\ \Omega_{M_p} &= 4069.01335^\circ/\text{centuries} \\ \Omega_{M_S} &= 1934.13784^\circ/\text{centuries} \end{aligned} \tag{21}$$

It is important to notice that the expressions (10),(16),(17) and (18) obtained by series expansion and truncated, contain all the important frequencies of the motion of the Moon. The combination of angles $\varphi_M, \varphi_{M_a}, \varphi_{M_p}, \varphi_{M_s}$ and the three rates (21) have been defined so that they correspond to the

most important features of its motion, known since Babylonian astronomy, namely: the orbital revolution around the Earth in a Lunar month (here we took the anomalistic month of 27.55 days as a reference) with Ω_{M_a}, the precession of its perigee with a period of about 8.85 years with Ω_{M_p} and the precession of its node with a period of about 18.6 years known as the Saros cycle with Ω_{M_S}. Finally the expression of $\mathbf{r}$ the position vector of the object itself in our non-rotating frame of reference is the following :

$$\mathbf{r} = \begin{pmatrix} \rho\cos\Phi \\ \rho\sin\Phi \\ z \end{pmatrix} = \begin{pmatrix} \rho\cos(\varphi+\varphi_E) \\ \rho\sin(\varphi+\varphi_E) \\ z \end{pmatrix} \tag{22}$$

with

$$\varphi_E = \Omega_\oplus t\ . \tag{23}$$

$\Omega_\oplus$ has already been defined, and corresponds to the daily frequency of rotation of the Earth, but to compare with the rates given in (21) we write it in the same units of degree/centuries:

$$\Omega_\oplus \sim 13185000^\circ/\text{centuries}. \tag{24}$$

2.5. The solar radiation pressure

The Solar radiation pressure perturbation derives from the following potential in the cannonball approximation ([19]):

$$V_{SRP} = C_r P_r\ AU^2\ \frac{A}{m}\ \frac{1}{|\mathbf{r}-\mathbf{r}_\odot|} \tag{25}$$

with C_r the reflectivity coefficient, depending on the optical properties of the space debris surface, taken equal to 1 in our study, P_r $=4.56\times10^{-6}\,\mathrm{N/m^2}$ is the radiation pressure for an object located at 1 AU the astronomical unit of distance, and $\frac{A}{m}$ the area-to-mass ratio with A the cross-section and m the mass.

Since this potential has the same shape as the *direct* part of the Solar potential (7), it is well defined and its treatment will be the same as this one, and therefore as precise.

2.6. Time dependence, frequencies and resonances

The introduction of the angles $(\varphi_E, \varphi_M, \varphi_{M_a}, \varphi_{M_p}, \varphi_{M_S})$ and their rates $(\Omega_\oplus, \Omega_M, \Omega_{M_a}, \Omega_{M_p}, \Omega_{M_S})$ in the previous sections is linked to the time-dependence of the Hamiltonian (4). This dependence on time is not desirable for a couple of reasons: first, for numerical integration purposes, having no time dependence is useful to check the accuracy of the integration through the preservation of the energy, and secondly for the normal form procedure we need to have these angles defined instead of time to see which combinations of them give rise to long periods variations in some quantities that we are interested in. We can do without this time dependence by introducing via canonical transformations an extended Hamiltonian which is not function of time itself but of the angles mentioned above and their conjugated momenta $(\rho, \varphi, z, \varphi_E, \varphi_M, \varphi_{M_a}, \varphi_{M_p}, \varphi_{M_S}, p_\rho, p_\varphi, p_z, J_E, J_M, J_{M_a}, J_{M_p}, J_{M_S})$, representing the same system and still named here H for simplicity:

$$\begin{aligned} H = {} & \frac{{p_\rho}^2}{2} + \frac{{p_\varphi}^2}{2r^2\sin^2\theta} + \frac{p_z^2}{2} \\ & + V(\rho,\varphi,z,\varphi_E,\varphi_M,\varphi_{M_a},\varphi_{M_p},\varphi_{M_S}) \\ & - \Omega_\oplus p_\varphi + \Omega_\oplus J_E + \Omega_M J_M + \Omega_{M_a} J_{M_a} \\ & + \Omega_{M_p} J_{M_p} + \Omega_{M_S} J_{M_S}, \end{aligned} \tag{26}$$

with

$$\begin{aligned} p_\rho &= \dot\rho \\ p_\varphi &= \rho^2(\dot\varphi + \Omega_\oplus) \\ p_z &= \dot z\ . \end{aligned} \tag{27}$$

We have now obtained the Hamiltonian (26) of our system without any other approximations than the ones made in truncating the series describing the position of Moon and the Sun. As explained these approximations still account for all the main dynamical features of the movement of the Moon and Sun. Before proceeding further to the normal form procedure, in order to make appear combinations of angles that are dynamically interesting, we expand the denominator of the potentials of the Moon (6), the Sun (7) and the SRP (25) in series. This is classically done by expanding these denominators with respect to the small ratios $\left|\frac{\mathbf{r}}{\mathbf{r}_\odot}\right|$ and $\left|\frac{\mathbf{r}}{\mathbf{r}_\mathbb{C}}\right|$ at order 2. After this necessary step, we can continue the modification of our Hamiltonian, to prepare it specifically to the study of the motion of objects around GEO.

2.7. Expansion around the geostationary radius

The full Hamiltonian (26) describes a system containing an object orbiting the Earth accounting for the different perturbations (i),(ii),(iii) without any other hypothesis or constraint so far. Since we are interested in the motion around the GEO region, we now make an expansion about the geostationary radius. Let us first introduce a few concepts.

2.7.1. Geostationary radius

The angular velocity of a particle in a circular motion around the Earth at a distance r considering only the potential of a spherical Earth $V_{GEO_0} = -\frac{\mu_\oplus}{r}$ is defined as :

$$\Omega(r) = \sqrt{\frac{1}{r}\frac{dV_{GEO_0}(r)}{dr}} = \sqrt{\frac{\mu_\oplus}{r^3}}. \tag{28}$$

The radius at which $\Omega = \Omega_\oplus$ is called the *geostationary radius*, r_c. With this definition $r_c = \rho_c = 42164.697\ km$. If a higher-order geopotential is considered, the value of the geostationary radius varies only of a few hundred meters, which is why we stick with this definition. We can then define $p_c = \rho_c^2\Omega_\oplus$, which is the angular momentum of a particle at ρ_c.

2.7.2. *Effective potential*

We also introduce the effective potential

$$V_{GEO_{eff}} = \frac{p_c^2}{2r^2} + V_{GEO_0}(r), \tag{29}$$

which describes the radial motion with constant angular momentum p_c.

2.7.3. *Epicyclic frequencies*

The frequencies of the radial and vertical small amplitude oscillations at GEO, κ_ρ and κ_z, are then defined as follows :

$$\begin{aligned} \kappa_\rho &= \sqrt{\frac{d^2 V_{GEO_{eff}}}{d\rho^2}}, \\ \kappa_z &= \sqrt{\frac{d^2 V_{GEO_{eff}}}{dz^2}}. \end{aligned} \tag{30}$$

Actually, if the effect of $C_{2,0}$ was not taken in account, in view of the radial symmetry we would simply have:

$$\kappa_\rho = \kappa_z = \sqrt{\frac{\mu_\oplus}{\rho_c^3}} = \Omega_\oplus.$$

In general, κ_ρ and κ_z are called *epicyclic frequencies*.

2.7.4. *Expansion of the Hamiltonian*

To complete the expansion of the Hamiltonian, we then introduce the variables $\delta\rho = \rho - \rho_c$ measuring the distance with respect to the geostationary radius ρ_c, and $J_\varphi = p_\varphi - p_c$ the difference in angular momentum with respect to the angular momentum at GEO p_c. We also introduce $\delta z = z$ to note that the expansion is done around $z = 0$. This change of variable is canonical, and the Hamiltonian is now a function of $(\delta\rho, \varphi, \delta z, \varphi_E, \varphi_M, \varphi_{M_a}, \varphi_{M_p}, \varphi_{M_S}, p_\rho, p_\varphi, p_z, J_E, J_M, J_{M_a}, J_{M_p}, J_{M_S})$. An expansion is necessary since the terms coming from the geopotential contain denominators which are not desirable for the reason mentioned in section 2.6. We therefore expand the Hamiltonian in $\delta\rho$ and δz, up to order 8.

2.8. Book-keeping process

At this point, to ease the process of expansion in series during the normal form procedure, let us introduce an important calculus artifice: the *book-keeping* coefficient [24] that helps keeping track of how small a given term in the Hamiltonian is. Our Hamiltonian is a sum of about 300 monomials at this point, which are all of different orders of smallness depending on their origin. The small parameters in our system are: $\mu_\odot$, $\mu_\leftmoon$, $C_{2,0}$, $C_{2,2}$ and $S_{2,2}$, P_r, the terms corresponding to the eccentricity and inclination of the orbit of the Moon and the Sun, and the terms corresponding to the precession of the perigee and node of the Moon. Among the terms corresponding to the Sun and the Moon, we consider even smaller the terms corresponding to correction of order 2 or more of the different elements describing their motion defined in section 2.4. We also consider small the following variables: $\delta\rho$, δz, J_φ. To each of these parameters we formally assigned a multiplicative book-keeping coefficient λ (which numerical value is set to 1 in computations). Different powers of λ are assigned to reflect each parameter's smallness, the higher the power, the smaller the parameter. For instance, the book-keeping process is chosen such that at order 0 in λ, the only terms in $(\delta\rho, p_\rho)$ and $(\delta z, p_z)$ present are $\frac{\kappa_\rho^2}{2}\delta\rho^2 + \frac{p_\rho^2}{2}$ and $\frac{\kappa_z^2}{2}\delta z^2 + \frac{p_z^2}{2}$, which are harmonic oscillators of frequency κ_ρ and κ_z respectively. This choice is made since this behavior is one of the things we want to highlight.

This process eases the expansions with respect to small parameters since we can now group all the terms in the Hamiltonian by their power of λ (also called order). Each term in the Hamiltonian has now a certain power of λ attached to it, and the Hamiltonian itself is a polynomial of order 10 in λ.

An important remark is that the book-keeping process is a little arbitrary, but the order in λ associated to a term during this process is not crucial for the success of the normal form procedure, especially at high order.

2.9. Action-angle variables

The final step before starting normalizing the Hamiltonian is to pass to action-angle variables via the following classical canonical change of variables:

$$\begin{aligned} \delta\rho &= \sqrt{\frac{2J_\rho}{\kappa_\rho}}\sin(\varphi_\rho), \\ \delta z &= \sqrt{\frac{2J_z}{\kappa_z}}\sin(\varphi_z), \\ p_\rho &= \sqrt{2\kappa_\rho J_\rho}\cos(\varphi_\rho), \\ p_z &= \sqrt{2J_z\kappa_z}\cos(\varphi_z). \end{aligned} \tag{31}$$

The Hamiltonian is now a function of $(\varphi_\rho, \varphi, \varphi_z, \varphi_E, \varphi_M, \varphi_{M_a}, \varphi_{M_p}, \varphi_{M_S}, J_\rho, J_\varphi, J_z, \ J_E, J_M, J_{M_a}, J_{M_p}, J_{M_S})$ and written in action-angle variables, ready to be normalized.

Remark: At this point it is useful to compare the actions defined in (31) to some Keplerian elements and Delaunay elements. Indeed $J_\rho + J_\varphi + J_z \sim L$, the Delaunay action equal to $\sqrt{\mu_\oplus a}$, a being the semi-major axis. The following relations also hold: $J_\rho \sim \frac{\sqrt{\mu_\oplus \rho_c}}{2}e^2$, $J_z \sim \frac{p_c}{2}\tan^2 i \sim \frac{p_c}{2}i^2$ for small i, and $J_\varphi = \mathrm{H} - p_c = \sqrt{\mu_\oplus a}\sqrt{1-e^2}\cos i - p_c$, H being here the Delaunay action.

3. FORCED EQUILIBRIUM

3.1. The normal form algorithm

The aim of the normal form procedure is to produce a good local approximation of the Hamiltonian, the *normal form*, that is easier to analyze.

This procedure is based on a sequence of near-identity canonical transformations. Such transformations, applied to a Hamiltonian $H(\mathbf{q},\mathbf{p})$ produce by definition a new Hamiltonian $K(\mathbf{Q},\mathbf{P})$ function of different variables but that still represents the same system, since $(\mathbf{Q},\mathbf{P})$ still satisfy Hamilton's equations of motion for K. Our goal here is to have a new Hamiltonian of the following form $H_{new}(\mathbf{Q},\mathbf{P}) = Z(\mathbf{Q},\mathbf{P}) + R(\mathbf{Q},\mathbf{P})$, Z being the normal form at any stage of the normalization process, and R the remainder supposed to be much smaller.

At the start the procedure, the Hamiltonian has the following form $H = H^{(0)} = Z_0 + \lambda H_1^{(0)} + \lambda^2 H_2^{(0)} + ...$, thanks to the book-keeping process. We then define a *module*, containing the terms desired in the normal form, Z_0 containing the terms in the original Hamiltonian of order 0 in λ is on purpose already in normal form due to the choice of book-keeping made. The sequence of canonical transformation is then done recursively via *Lie series* [8, 9]. For one given order of normalization r, a new Hamiltonian is obtained as $H^{(r)} = exp(L_{\chi_r})H^{(r-1)}$, with $L_\chi = \{.,\chi\}$ the Poisson bracket with χ, defined as follows $\{f,g\} = \sum_{i=1}^{n} \frac{\partial f}{\partial q_i}\frac{\partial g}{\partial p_i} - \frac{\partial f}{\partial p_i}\frac{\partial g}{\partial q_i}$ and $exp(L_\chi) = \sum_{i=0}^{\infty} \frac{1}{k!} L_\chi^k$ is the Lie series operator [2]. This infinite series is truncated at one given order which is the final order of normalization. At this order of normalization r, all of the terms of order less than r in λ will be in normal form. The only unknown in this process is the *generating function* χ_r, that is found by solving at each normalization order the *homological equation* $\{Z_0,\chi_r\} = -\lambda^r \tilde{H}_r^{(r-1)}$, where $\tilde{H}_r^{(r-1)}$ represents the terms of $H^{(r-1)}$ of order in λ higher than r *not* belonging to the module. Different choices of module can be done and lead to different normalization schemes.

Coming back to our Hamiltonian, after performing (31), it is composed of monomials of the following form:

$$\begin{aligned}&\lambda^r J_\rho^{m_1} p_\varphi^{m_2} J_z^{m_3} J_E^{m_4} J_M^{m_5} J_{M_a}^{m_6} J_{M_p}^{m_7} J_{M_S}^{m_8} \\ &\quad\times \cos(k_1\varphi_\rho + k_2\varphi + k_3\varphi_z + k_4\varphi_E \\ &\quad + k_5\varphi_M + k_6\varphi_{Ma} + k_7\varphi_{Mp} + k_8\varphi_{Ms}),\end{aligned} \tag{32}$$

m_i, k_i and r being integers. One can show [24] that the terms that will be normalized by the algorithm will have at their denominator terms of the form $k_1\kappa_\rho + k_3\kappa_z + k_4\Omega_\oplus + k_5\Omega_M + k_6\Omega_{Ma} + k_7\Omega_{Mp} + k_8\Omega_{Ms}$ (there is no k_2 since the frequency associated to φ is 0). If there exist a combination of the k_i that makes this quantity close to 0, the term will be a *small divisor*. This has to be avoided for the convergence of the series, and therefore the resonant module is defined as the set of terms in the Hamiltonian such that $\{k_1 + k_3 + k_4 \approx 0\}$ since the frequencies κ_ρ, κ_z and $\Omega_\oplus$ are very close to each other ($\sim 1/\text{day}$).

This normalization is done up to order 4, and we obtain a new Hamiltonian function $H^{(4)}$ of a new set of variables $(\varphi_\rho^{(4)}, \varphi^{(4)}, \varphi_z^{(4)}, \varphi_E^{(4)}, \varphi_M^{(4)}, \varphi_{Ma}^{(4)}, \varphi_{Mp}^{(4)}, \varphi_{MS}^{(4)}, J_\rho^{(4)}, J_\varphi^{(4)}, J_z^{(4)}, J_E^{(4)}, J_M^{(4)}, J_{Ma}^{(4)}, J_{Mp}^{(4)}, J_{MS}^{(4)}) = (\mathbf{q}^{(4)}, \mathbf{p}^{(4)})$. One can express the original variables $(\mathbf{q},\mathbf{p})$ in function of these via the following relation:

$$(\mathbf{q},\mathbf{p}) = exp(L_{\chi_4}) \circ ... \circ exp(L_{\chi_1})(\mathbf{q}^{(4)}, \mathbf{p}^{(4)}), \tag{33}$$

We drop the superscript in the following for simplicity.

3.2. Slow and fast variables

We now drop the remainder supposed to be small and consider only the normal form. It has the following features : the only terms present at order 0 in the book-keeping parameter λ are $J_\rho\kappa_\rho + J_z\kappa_z + J_E\Omega_\oplus + J_M\Omega_M + J_{M_a}\Omega_{Ma} + J_{M_p}\Omega_{Mp} + J_{M_S}\Omega_{Ms}$, there are no terms at order 1 in λ, and at order 2, a few terms are present and they contain among others, the following trigonometric arguments : $\varphi_\rho - \varphi - \varphi_E + \varphi_M$. This angle is associated to the frequency $\kappa_\rho - \Omega_\oplus + \Omega_M$ which is comparable to Ω_M since $\kappa_\rho \approx \Omega_\oplus$, and therefore this is a slow angle compared to φ_E for instance. This motivates the following canonical change of variable to make appear the slow and fast variables:

$$\begin{aligned}\varphi_{ec} &= \varphi_\rho - \varphi - \varphi_E + \varphi_M, & J_{ec} &= J_\rho, \\ \varphi_R &= \varphi, & J_R &= J_\varphi + J_{ec} + J_{in}, \\ \varphi_{in} &= \varphi_z - \varphi - \varphi_E, & J_{in} &= J_z, \\ \varphi_e &= \varphi_E, & J_e &= J_E + J_\rho + J_z, \\ \varphi_m &= \varphi_M, & J_m &= J_{\varphi_M} - J_\rho, \\ \varphi_{ma} &= \varphi_{Ma}, & J_{ma} &= J_{\varphi_{Ma}}, \\ \varphi_{mp} &= \varphi_{Mp}, & J_{mp} &= J_{\varphi_{Mp}}, \\ \varphi_{ms} &= \varphi_{Ms}, & J_{ms} &= J_{\varphi_{Ms}}.\end{aligned} \tag{34}$$

Here, J_{ec} is an action that is related to the eccentricity vector, and J_{in} and action related to the inclination vector via the relations expressed in section 2.9. φ_{ec} and φ_{in} are now slow angles compared with φ_e.

3.3. Poincaré variables

The Hamiltonian obtained after performing (34) contains terms resembling a forced pendulum in the couple of variables (J_{ec}, φ_{ec}) and (J_{in}, φ_{in}) and motivates a canonical

[2] The Lie series have among other advantages the ones of being very practical computationally speaking, in the sense that they involve only sums, products and derivatives of functions, easily programmable in an algebraic manipulator. They also do not involve composition of function since the Lie operator is directly applied to the Hamiltonian or the variables themselves.

change of variables to rectangular Poincaré variables :

$$\begin{aligned} x_e &= \sqrt{2J_{ec}}\sin(\varphi_{ec}),\\ y_e &= \sqrt{2J_{ec}}\cos(\varphi_{ec}),\\ x_i &= \sqrt{2J_{in}}\sin(\varphi_{in}),\\ y_i &= \sqrt{2J_{in}}\cos(\varphi_{in}). \end{aligned} \tag{35}$$

By selecting in the resulting Hamiltonian the terms only depending on (x_e, y_e, x_i, y_i), we get a toy model, for which we can solve for the forced equilibrium position.

3.4. Forced equilibrium

The forced equilibrium of this toy model is the following [3]:

$$\begin{aligned} x_{ef} &= -0.138785,\\ y_{ef} &= -0.000012,\\ x_{if} &= -0.231519,\\ y_{if} &= 0.042744. \end{aligned} \tag{36}$$

By combining (35) and the relations from section 2.9, we can translate these values in eccentricity and inclination :

$$\begin{aligned} e_{forced} &\sim \sqrt{\frac{x_{ef}^2 + y_{ef}^2}{\sqrt{\rho_c \mu_\oplus}}},\\ i_{forced} &\sim \arctan\left(\sqrt{\frac{x_{if}^2 + y_{if}^2}{p_c}}\right). \end{aligned} \tag{37}$$

This corresponds to a forced eccentricity of 0.113 and a forced inclination of $10.88°$ for an $\frac{A}{m} = 10\,\mathrm{m}^2/\mathrm{kg}$. This is in accordance with the values found in [18, 4, 17].

3.5. Expansion around the forced equilibrium

Numerically integrating the equations of motion given by the full Hamiltonian starting at equilibrium (36) yields variations of up to 10% for (x_e, y_e, x_i, y_i). This shows the need for a refined equilibrium. To find it, we expand our Hamiltonian around $(x_{ef}, y_{ef}, x_{if}, y_{if})$ by introducing new variables :

$$\begin{aligned} \delta x_e &= x_e - x_{ef},\\ \delta y_e &= y_e - y_{ef},\\ \delta x_i &= x_i - x_{if},\\ \delta y_i &= y_i - y_{if}. \end{aligned} \tag{38}$$

Then we put the Hamiltonian in new action-angle variables. For this, a diagonalization of a toy model of the Hamiltonian restricted to the $(\delta x_e, \delta y_e, \delta x_i, \delta y_i)$ variables is done. The transformation $(\delta x_e, \delta y_e, \delta x_i, \delta y_i) \to (q_1, p_1, q_2, p_2)$ obtained is applied to the whole Hamiltonian. Then to finish the transformation to action-angle variables we do the following canonical transformation :

$$\begin{aligned} q_k &\to \sqrt{J_k} e^{i\varphi_k},\\ p_k &\to -i\sqrt{J_k} e^{-i\varphi_k}. \end{aligned} \tag{39}$$

To refine the equilibrium, a new normalization of this Hamiltonian in action-angle variables is needed.

3.6. Second normalization

This time, we want to eliminate very precise terms, the terms that cause the non-constancy of $(\delta x_e, \delta y_e, \delta x_i, \delta y_i)$. They are terms linear in $(\delta x_e, \delta y_e, \delta x_i, \delta y_i)$ and actually contain *small divisors*. We therefore define a threshold up to which we keep the terms with a given small divisor so that they contribute to the dynamics of the normal form. The new normalization will eliminate the other ones up to second order in book-keeping.

3.7. Nature of the forced equilibrium

Back-transforming from the action-angle variables $(J_1, \varphi_1, J_2, \varphi_2)$ with which the Hamiltonian was normalized to the $(\delta x_e, \delta y_e, \delta x_i, \delta y_i)$ and numerically integrating the results, the variations are smaller by one order of magnitude.

We now consider those variations small enough, and therefore the new $(\delta x_e, \delta y_e, \delta x_i, \delta y_i)$ as quasi-constants. Via the generating function of the transformation as explained shown in (33), we can then express the old $(\delta x_e, \delta y_e, \delta x_i, \delta y_i)$ in function of these new ones, considered as constant (equal to their refined equilibrium values) and obtain an expression of them directly as functions of time. The forced equilibrium is then a lower dimensional object containing a combination of five distinct frequencies, which are the ones defined in section (2.6).

The nature of the forced equilibrium is clear on Figure 1: the inner orbit (the real one being the blue) starting at the equilibrium is a quasi-periodic orbit exhibiting small variations in the (x_e, y_e) variables, and even the normal form (in purple) captures this behavior, albeit with smaller variations, by virtue of its definition. The long-term evolution of the eccentricity and inclination starting at the equilibrium is shown on Figure 3 and 4 respectively. The eccentricity for instance varies about 4% with respect to its initial value.

3.8. Analytical expression for the time evolution at equilibrium of the original cylindrical coordinates

From the original $(\delta x_e, \delta y_e, \delta x_i, \delta y_i)$ variables (prior to normalization) expressed in function of time we can come back to (ρ, φ, z) using one after another: (38), (35), (34), the generating function of the first normal form as in (33) and finally (31), and express them in function of time only too. This

[3] It is important to note that these value are computed in our units where the time unit is 1 day (86 400 s) and the distance unit 86 400 km.

gives us an analytical formula of our original cylindrical coordinates at the forced equilibrium, since it their expression depends then on time only.

It is important to note that during our calculations, we actually also carry along the Hamiltonian the original variables, expressed at each stage in function of the variables used in the Hamiltonian at that stage. So at this final step, we just substitute in (ρ, φ, z) that are at this time expressed in function of $(\delta x_e, \delta y_e, \delta x_i, \delta y_i)$, their expression in function of time. This approach is computationally more efficient. The remark of the previous paragraph was to show the reader how it is possible to obtain the original variables as function of time in a general case, and although that approach is less computationally efficient, it is still feasible.

The analytical formulas for (ρ, φ, z) and any other set of elements that can be used to describe the motion at equilibrium typically contain about a thousand terms and therefore cannot be shown here, but the results can be seen in Figure 2. The error in radial distance ρ over 10000 days is less than 1.2% and even less than 0.6% for 1000 days.

4. CONCLUSION

We studied the long-term evolution of objects around the GEO region, including high area-to-mass ratio objects. For this purpose we started from a Hamiltonian model describing the evolution of an object at GEO accounting for all major perturbations including the solar radiation pressure. We normalized this Hamiltonian to find the forced equilibrium of the system. This allowed us to show that this equilibrium is actually a quasi-periodic orbit, and that an object put there will see its elements vary over time. We then derived analytical expressions for the evolution of our original variables at this equilibrium. These expressions can be transcribed to any set of elements allowing for fast calculations regarding the evolution of an object at the equilibrium.

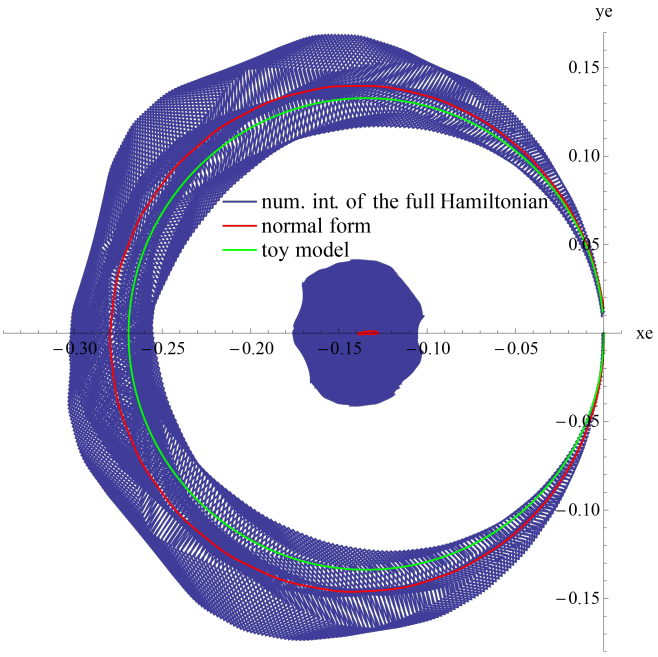

Fig. 1: Illustration of the usefulness of the normal form procedure: Representation of two different geostationary orbits (duration 1 year) with three different methods (Numerical integration of the full Hamiltonian (blue), normal form (red), and the toy model (green) derived from the normal form to calculate the forced equilibrium) for the couple of variables (x_e, y_e). The outer orbit corresponds to initial conditions $e = 0, i = 0$, the interior one to the forced equilibrium $e \approx e_{forced} = 0.113, i \approx i_{forced} = 10.88°$. The debris considered has an $\frac{A}{m}$ of $10\,\mathrm{m}^2/\mathrm{kg}$.
We notice that for the outer orbit, the normal form and the toy model capture the long term dynamics without the daily variations, illustrating the principle of averaging. For the forced equilibrium, we clearly see that it is actually a pseudo equilibrium since variations do exist for the real (blue) orbit. The normal form exhibits tiny variations since it is an expansion built to find this equilibrium, and the toy model variations are actually invisible since the forced equilibrium is a fixed point for this model.

5. REFERENCES

[1] C.C. Chao, *Applied Orbit Perturbation and Maintenance*, AIAA, November 2005.

[2] L. Anselmo and C. Pardini, "Long-Term Evolution of High Earth Orbits : Effects of Direct Solar Radiation Pressure and Comparison of Trajectory Propagators," Tech. Rep., 2007.

[3] C.C. Chao and J.M. Baker, "On the propagation and control of geosynchronous orbits," *Journal of the Astronautical Sciences*, vol. 31, pp. 99–115, March 1983.

[4] C.C. Chao, "Analytical Investigation of GEO Debris with High Area-to-Mass Ratio," in *AIAA/AAS Astrodynamics Specialist Conference and Exhibit*, Reston, Virigina, August 2006, pp. 1–9, AIAA.

[5] S. Valk, A. Lemaître, and L. Anselmo, "Analytical and semi-analytical investigations of geosynchronous space debris with high area-to-mass ratios," *Advances in Space Research*, vol. 41, no. 7, pp. 1077–1090, January 2008.

[6] A.J. Rosengren and D.J. Scheeres, "Long-term dynamics of high area-to-mass ratio objects in high-Earth orbit," *Advances in Space Research*, vol. 52, no. 8, pp. 1545–1560, October 2013.

[7] O. Montenbruck and E. Gill, *Satellite Orbits*, vol. 134, Springer Berlin Heidelberg, July 2000.

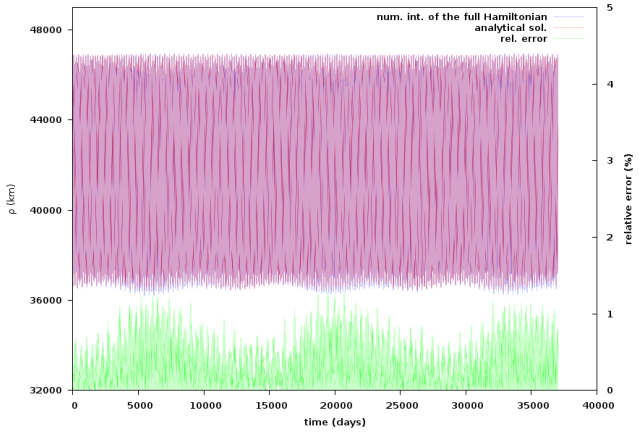

Fig. 2: Time evolution of ρ the planar distance, at the forced equilibrium, for 36525 days (100 years). Numerical integration of the full Hamiltonian (blue), time-explicit analytical model (purple), and difference between the two (yellow). The relative error is less than 1.3%.

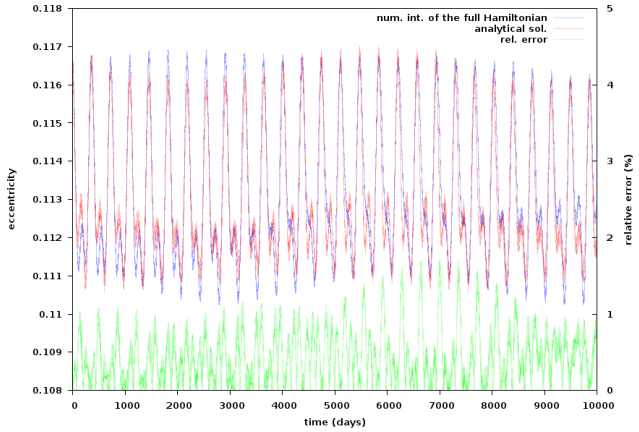

Fig. 3: Time evolution of the eccentricity, at the forced equilibrium, for 10000 days ($\approx$ 27.4 years). Numerical integration of the full Hamiltonian (blue), time-explicit analytical model (purple), and difference between the two (yellow). The relative error is less than 1.8%.

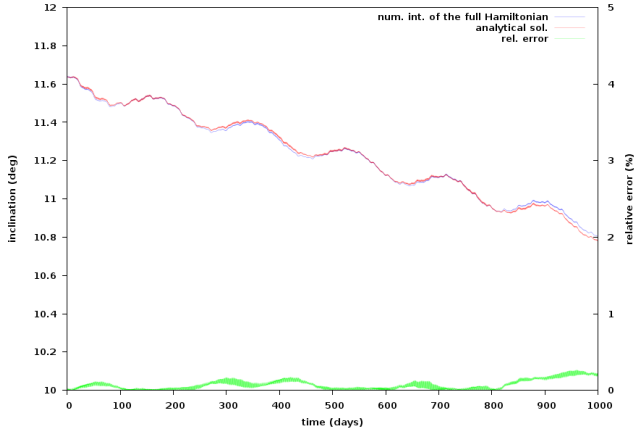

Fig. 4: Time evolution of the inclination, at the forced equilibrium, for 1000 days ($\approx$ 2.7 years). Numerical integration of the full Hamiltonian (blue), time-explicit analytical model (purple), and difference between the two (yellow). The relative error is less than 0.2%.

[8] G.-I. Hori, "Theory of general perturbation with unspecified canonical variable," *Publications of the Astronomical Society of Japan*, vol. 18, no. 4, pp. 287–296, 1966.

[9] A. Deprit, "Canonical transformations depending on a small parameter," *Celestial Mechanics*, vol. 1, no. 1, pp. 12–30, March 1969.

[10] NASA, "Orbital Debris Quarterly News," January 2015.

[11] "IADC Space Debris Mitigation Guidelines (rev. 1)," Tech. Rep., 2007.

[12] L. Anselmo and C. Pardini, "Space debris mitigation in geosynchronous orbit," *Advances in Space Research*, vol. 41, no. 7, pp. 1091–1099, 2008.

[13] T. Schildknecht et al., "Optical observations of space debris in GEO and in highly-eccentric orbits," vol. 34, pp. 901–911, 2004.

[14] J.-C. Liou and J.K. Weaver, "Orbital Dynamics of High Area-To-Mass Ratio Debris and Their Distribution in the Geosynchronous Region," in *4th European Conference on Space Debris*, D. Danesy, Ed., August 2005, vol. 587 of *ESA Special Publication*, p. 285.

[15] T. Schildknecht, "Optical surveys for space debris," *The Astronomy and Astrophysics Review*, vol. 14, no. 1, pp. 41–111, jan 2007.

[16] L. Anselmo and C. Pardini, "Orbital Evolution of Geosynchronous Objects with High Area-To-Mass Ratios," in *4th European Conference on Space Debris*, D. Danesy, Ed., August 2005, vol. 587 of *ESA Special Publication*, p. 279.

[17] D. Casanova, A. Petit, and A. Lemaître, "Long-term evolution of space debris under the J2 effect, the solar radiation pressure and the solar and lunar perturbations," *Celestial Mechanics and Dynamical Astronomy*, vol. 123, no. 2, pp. 223–238, October 2015.

[18] A.J. Rosengren, D.J. Scheeres, and J.W. McMahon, "The classical Laplace plane as a stable disposal orbit for geostationary satellites," *Advances in Space Research*, vol. 53, no. 8, pp. 1219–1228, apr 2014.

[19] T. Kubo-Oka and A. Sengoku, "Solar radiation pressure model for the relay satellite of SELENE," *Earth, Planets, and Space*, vol. 51, pp. 979–986, 1999.

[20] C. Hubaux and A. Lemaître, "The impact of Earths shadow on the long-term evolution of space debris," *Celestial Mechanics and Dynamical Astronomy*, vol. 116, no. 1, pp. 79–95, May 2013.

[21] S. Valk, A. Lemaître, and F. Deleflie, "Semi-analytical theory of mean orbital motion for geosynchronous space debris under gravitational influence," *Advances in Space Research*, vol. 43, no. 7, pp. 1070–1082, 2009.

[22] W. M. Kaula, *Theory of satellite geodesy. Applications of satellites to geodesy*, 1966.

[23] F.G. Lemoine et al., "The development of the joint NASA GSFC and the National Imagery and Mapping Agency (NIMA) geopotential model EGM96," 1998.

[24] C. Efthymiopoulos, "Canonical perturbation theory; stability and diffusion in Hamiltonian systems: applications in dynamical astronomy," *Workshop Series of the Asociacion Argentina de Astronomia*, vol. 3, pp. 3–146, 2011.